Published in final edited form as:
Neuron. 2008 November 26; 60(4): 698–708. doi:10.1016/j.neuron.2008.09.013.

Distinct mechanisms for top-down control of neural gain and sensitivity in the owl optic tectum

Daniel E. Winkowski* and **Eric I. Knudsen**
Stanford University Medical Center, Neurobiology Department, 299 Campus Drive West, Stanford, CA 94305-5125

Summary

We demonstrate that distinct mechanisms of top-down control regulate, respectively, the sensitivity and gain of sensory responses in the owl's optic tectum (OT). Electrical microstimulation in the forebrain gaze-control area, the arcopallial gaze field (AGF), results in a space-specific regulation of sensory responses in the OT. AGF microstimulation increases the responsiveness of OT neurons representing stimuli at the same location as that represented at the AGF site. We show that the mechanism that underlies this effect operates focally to enhance neuronal sensitivity and to improve tuning consistency and spatial resolution. At the same time, AGF microstimulation decreases the responsiveness of OT neurons representing stimuli at all other locations. The mechanism that underlies this effect operates globally to modulate neuronal gain. The coordinated action of these different mechanisms can account for many of the reported effects of spatial attention on neural responses in monkeys and on behavioral performance in humans.

Introduction

A fundamental component of attention is the top-down regulation of the responsiveness of sensory neurons, predominantly in high-order areas of the brain (Desimone and Duncan, 1995; Maunsell and Cook, 2002; Moore et al., 2003; Reynolds and Chelazzi, 2004; Knudsen, 2007). When an animal directs its attention either toward a location in space or toward a particular stimulus, the responsiveness of high-order neurons that are tuned to the location and features of the stimulus is increased. This dynamic and selective enhancement of sensory responses is thought to improve the analysis and evaluation of the attended stimulus (Moran and Desimone, 1985; Spitzer et al., 1988).

The properties of top-down regulation of sensory responsiveness have been explored at many levels of visual, auditory and somatosensory processing in animals that have been trained to attend to specific stimuli (Bauer et al., 2006; Desimone and Duncan, 1995; Fritz et al., 2007; Reynolds and Chelazzi, 2004; Steinmetz et al., 2000). In these studies, the modulation of sensory responsiveness by attention is measured as the difference between neural responses when an animal attends towards a stimulus versus when it attends away from the same stimulus. All studies report a relative increase in neural responses when the animal attends toward the

Corresponding Author: Daniel E. Winkowski, University of Maryland, Institute for Systems Research, 1103 A.V. Williams Building, College Park, MD 20742, dwinkows@umd.edu.
*Current Address: Daniel E. Winkowski, University of Maryland, Institute for Systems Research, 1103 A.V. Williams Building, College Park, MD 20742, dwinkows@umd.edu

stimulus. One explanation for this effect is a mechanism that increases the responsiveness of neurons tuned to the selected location or features of a stimulus. Another possibility, however, is that two different top-down mechanisms regulate neural responsiveness: one increases the responsiveness of neurons to the attended stimulus and a second mechanism decreases the responsiveness of neurons to non-attended stimuli. When the effects of attention are measured in the traditional way, the difference between these possibilities cannot be resolved.

Recently, an experimental paradigm has been developed that allows these alternative possibilities to be disambiguated for spatial attention. The paradigm takes advantage of the tight linkage that exists between gaze control and spatial attention. When humans make a saccadic eye movement to a new location, behavioral sensitivity to stimuli at that location increases in the tens of milliseconds before the eyes move to that location (Hoffman and Subramaniam, 1995; Shepherd et al., 1986), suggesting that the intention to move the eyes shifts spatial attention to the endpoint of the impending saccade. The linkage between gaze control and spatial attention has also been demonstrated in monkeys: When weak electrical microstimulation is applied to a region of the forebrain that controls the direction of gaze (frontal eye fields; FEF), monkeys become behaviorally more sensitive to stimuli presented at the location represented at the site of microstimulation (Moore and Fallah, 2001; Moore and Fallah, 2004). At the same time, the responsiveness of visual cortical neurons in V4, a high-order area in the monkey's visual pathway, is selectively regulated such that neurons with receptive fields that include the location represented by the FEF microstimulation site, increase their responses to visual stimuli (Armstrong et al., 2006; Armstrong and Moore, 2007; Moore and Armstrong, 2003). This selective increase in neural responses in V4 mimics the increases recorded in V4 in monkeys trained to voluntarily direct their attention to stimuli (Desimone and Duncan, 1995; Reynolds and Chelazzi, 2004).

We have applied this microstimulation paradigm to barn owls. In our paradigm, the owl's forebrain gaze-control area, the AGF, is electrically microstimulated while sensory responses are monitored in the optic tectum (OT) as the animal rests passively (Winkowski and Knudsen, 2006; Winkowski and Knudsen, 2007). The AGF is the avian equivalent of the mammalian FEF (Knudsen et al., 1995). In behaving owls, inactivation of the AGF disrupts gaze saccades that are guided by working memory (Knudsen and Knudsen, 1996), as does inactivation of the FEF in behaving monkeys (Dias and Segraves, 1999). The OT is the avian equivalent of the mammalian superior colliculus. In monkeys, the superior colliculus has been shown to be critically involved in stimulus selection and attention tasks (McPeek and Keller, 2004; Müller et al., 2005). The microstimulation paradigm has revealed an array of effects on sensory responses in the OT of passive owls (Winkowski and Knudsen, 2006; 2007) that mimic the effects of FEF microstimulation on sensory responses in the visual cortex of monkeys (Armstrong and Moore, 2006; 2007). These effects include the highly space-specific regulation of neuronal responsiveness, sharpening of spatial receptive fields, and shifts in spatial receptive fields toward the location encoded by the forebrain stimulation site. Although it is unlikely that electrical microstimulation of forebrain gaze fields in a passive animal activates all of the mechanisms that operate in an animal that is attending voluntarily, it is highly plausible that the top-down mechanisms that are indeed engaged under these conditions are also engaged in behaving animals.

In the current study, we exploit the forebrain gaze field microstimulation paradigm to isolate the effects of two distinct mechanisms for top-down control of sensory responsiveness: one mechanism enhances neural sensitivity and spatial resolution, and another regulates neural response gain. The mechanisms were isolated with this paradigm because sensory response properties could be compared without (baseline) and with activating the top-down signal, and because the OT contains a topographic map of sensory space so that the effects of microstimulation could be measured both at OT sites that represent the same location in space

as that represented at the forebrain stimulation site (analogous to "attend-toward") and at OT sites that represent other locations in space (analogous to "attend-away"). The elucidation of two distinct mechanisms for top-down control resolves a long-standing controversy about whether top-down signals modulate either the gain or the sensitivity of sensory responses (Kauramäki et al., 2007; Martinez-Trujillo and Treue, 2002; Reynolds et al., 2000; Williford and Maunsell, 2006); they do both.

AGF microstimulation has been shown to modulate auditory as well as visual responses in the OT (Winkowski and Knudsen, 2007). In this study, we focus on the modulation of auditory responses. The auditory system derives stimulus location from auditory localization cues. The dominant localization cues are interaural time differences (ITDs), which correspond to the location of a stimulus in azimuth, and high frequency interaural level differences (ILDs), which for barn owls correspond to the location of a stimulus in elevation, due to a vertical asymmetry in the directional sensitivities of the ears. The spatial tuning of neurons in the AGF and OT was measured as their tuning to the ITD and ILD of broadband noise bursts presented through earphones. In characterizing the effects of AGF microstimulation on auditory responses, we concentrated on the representation of stimuli along the azimuthal dimension, therefore, on responses as a function of ITD.

RESULTS

Definition of aligned and nonaligned AGF-OT sites

We applied microstimulation to the medial portion of the AGF where units respond to auditory stimuli, a region referred to as the auditory AGF (AGFa). Units in the AGFa are tuned to both ITD and ILD, and neighboring units are tuned to approximately the same values of ITD and ILD, reflecting a clustered representation of auditory space (Cohen and Knudsen, 1995; Winkowski and Knudsen, 2007). After determining the best ITD and best ILD for a stimulation site centered within an AGFa cluster (see Experimental Procedures), we measured the minimum electrical stimulation current necessary to induce a saccadic eye movement (> 55 μA at all sites). Microstimulation current levels in the AGFa were kept below these levels (≤40 μA) in all experiments.

The definition of "aligned" versus "nonaligned" AGFa-OT sites was established in previous studies, based on the enhancing or suppressing effects of AGFa microstimulation on OT responsiveness (Winkowski and Knudsen, 2007). Aligned OT sites exhibit best ITDs within 22 μs (approximately 9° azimuth; the relationship between ITD and stimulus azimuth for barn owls is approximately 2.5 μs/°; see Olsen et al., 1989) of the best ITD at the AGFa stimulation site and best ILDs within 10 dB of that at the AGFa stimulation site. Nonaligned OT sites are those that exhibit either a best ITD or a best ILD that differs from those at the AGFa site by more than these values. Single unit and multiunit sites produced similar results and are presented together.

Effects on sound level-response functions in the OT

Aligned AGFa-OT sites—The effects of AGFa microstimulation on the responsiveness of an OT unit with an aligned receptive field are shown in Figure 1A. The receptive field measured at the AGFa stimulation site was centered at an ITD of −32 μs (negative ITD values indicate left ear leading) and at an ILD of −4 dB (negative ILD values indicate left ear greater); the receptive field at the OT site was centered at an ITD of −21 μs and at an ILD of −4 dB. Electrical microstimulation (8 μA) was applied to the AGFa, for 25 ms, just prior to the presentation of sound on randomly interleaved trials, as the tuning of the OT unit to ITD (sound level = −60 dB) was measured; trials in which only the AGFa was microstimulated were interleaved with these trials. Without AGFa stimulation, the OT unit responded to an ITD of −20 μs with an

average rate of 60 spikes/s. With AGFa stimulation, the tuning of the OT unit shifted to −23 μs ITD, and it responded to an ITD of −20 μs with an average rate of 75 spikes/s (response increase = 25%; $p < 0.05$). The shift in the best ITD of the OT site toward the best ITD of the AGFa stimulation site was significant (paired t-test; $p<0.01$); this effect has been described previously (Winkowski and Knudsen, 2006; Winkowski and Knudsen, 2007). AGFa microstimulation increased responses only to sounds within a limited portion of the unit's receptive field and did not affect responses to sounds outside of the receptive field ($p > 0.1$). There was no effect of AGFa microstimulation alone on the activity of this unit; the absence of an effect of AGFa microstimulation alone on OT neural activity has been documented previously (Winkowski and Knudsen, 2006; Winkowski and Knudsen, 2007).

To determine whether the ITD-specific increase in responsiveness induced by AGFa microstimulation was due to an increase in sensitivity or an increase in response gain, we measured the effect of stimulus sound level (holding ITD at −20 μs and ILD at −4 dB) on unit responses with and without AGFa microstimulation (Fig. 1B); this test is analogous to a contrast-response function for a visual unit. AGFa microstimulation had no effect on OT unit responses to sound levels below −75 dB, dramatically increased responses to sound levels of −75 to −65 dB, and had little or no effect on responses to sound levels above −60 dB. AGFa stimulation shifted the level-response function to the left, but did not change baseline activity ($p=0.3$, t-test), the maximum response rate ($p=0.2$, t-test), or the slope of the level-response function ($p=0.4$, t-test). Thus, for this AGFa -OT pair, AGFa microstimulation increased the sensitivity of the OT unit, but did not change the gain of its response.

To examine the consistency of the effect of AGFa microstimulation on level-response functions at aligned sites in the OT, we compared parameters of sigmoidal curves, fit to level-response functions with and without AGFa microstimulation, for a population of aligned AGFa-OT sites ($n = 57$, 10 single units). The parameters derived from these curves were: baseline activity, maximum response, sound level for a half-maximum response, and maximum slope. These parameters were compared with and without AGFa microstimulation using a modulation index: the difference in a parameter value divided by the sum of the parameter values (see Experimental Procedures). Increases or decreases of each response parameter were observed at subsets of OT sites (Fig. 1C). Across the population, however, the only consistent effect of AGFa microstimulation was a decrease in the sound level for a half-maximum response (Fig. 1C; $p < 0.02$, Wilcoxon signed rank test), indicating an increase in unit sensitivity without a change in response gain. Commensurate with this effect, AGFa stimulation also decreased response thresholds by a median value of 1.45 dB (Fig. 1E, $p < 10^{-4}$, signed rank test; see Experimental Procedures). In contrast, AGFa stimulation alone did not consistently alter spontaneous activity (stimulation-alone condition), which changed nominally from 4.3 ± 7.2 s.d. sp/s to 6.5 ± 9.1 sp/s ($p = 0.09$, Wilcoxon signed rank test).

Population average level-response functions, with and without AGFa microstimulation, documented the same effect (Fig. 1D, upper panel). Level-response functions were normalized to the maximum response without AGFa microstimulation and then were averaged together. Differences between the average level-response functions with and without AGFa stimulation revealed an average increase in OT responses to sound levels from 5 dB below threshold to 25 dB above threshold (Fig. 1D, lower panel; $p<0.05$). Thus, on average, AGFa microstimulation increased the sensitivity of aligned OT neurons by decreasing their response thresholds and shifting their level-response functions to the left.

Nonaligned *AGFa* -OT sites—The effect of AGFa microstimulation on the responsiveness of OT units at nonaligned sites was fundamentally different from that at aligned sites (Fig. 2). An example of the effect at a single, nonaligned OT site is shown in Fig. 2A,B. The receptive field measured at the AGFa stimulation site was centered at an ITD of +38 μs (see Fig 2A) and

at an ILD of +1 dB. The receptive field at the OT site was centered at an ITD of +10 μs (AGFa-OT difference = 11° azimuth) and at an ILD of +6 dB. AGFa microstimulation caused a 35% reduction in responses to sounds centered in the receptive field (Fig. 2A). The magnitude of response suppression increased proportionately with the strength of the response both across the receptive field (Fig. 2A) and across sound levels (Fig. 2B). AGFa stimulation decreased both the slope of the level-response function and the maximum response at the site (Fig. 2B).

Across the population of nonaligned AGFa -OT sites (n = 53, 9 single units), AGFa microstimulation exerted similar effects. AGFa microstimulation had no systematic effect on baseline activity or on the sound level for a half-max response (Fig. 2C), nor did it affect average spontaneous activity (stimulation-alone condition): 3.5 ± 4.1 s.d. sp/s without AGFa microstimulation and 3.3 ± 5.2 with AGFa microstimulation ($p > 0.5$, Wilcoxon signed rank test). Instead, it consistently decreased the slopes of level-response functions and decreased maximum response rates (Fig. 2C). AGFa microstimulation also increased response thresholds by a median value of 0.8 dB (Fig. 2E, $p < 0.01$, signed rank test). Population average level-response functions confirmed the results from curve fitting (Fig. 2D). They indicated a modest but significant effect of AGFa microstimulation on response thresholds and a suppressive effect that increased and then plateaued with increasing sound levels above threshold (Fig. 2D, lower panel).

Effect on response and tuning consistency

AGFa microstimulation did not change the consistency of auditory responses for either aligned or nonaligned OT sites. Response consistency was quantified as the ratio of response variance to response mean (Fano factor; see Experimental Procedures). Fano factors were computed for responses to stimuli centered in the OT receptive fields, with and without AGFa microstimulation. A modulation index was used to compare the values for the Fano factors with and without AGFa microstimulation. For aligned sites, the median change in Fano factor with AGFa microstimulation was 0.07 ($p > 0.1$, signed rank test). For nonaligned sites the median change in Fano factor was −0.06 ($p > 0.1$, signed rank test).

In contrast, AGFa microstimulation did alter the consistency of OT unit tuning to ITD. Tuning consistency was quantified as the inverse of the variance of best ITD values (Fig. 3A, open circles along abscissa), each computed from responses to a single set of ITD stimuli, across 15 sets of ITD stimuli (Fig. 3A, curves). The variances of best ITDs, measured without (Fig. 3A, top) and with AGFa microstimulation (Fig. 3A, bottom), were compared. For the aligned AGFa -OT sites, illustrated in Fig. 3A (top and bottom), the variance in best ITD across repeated measures decreased from 32 to 8 with AGFa microstimulation ($p < 0.01$, F-test for equal variance).

The effect of AGFa microstimulation on tuning consistency was evaluated across the population of AGFa -OT sites with a consistency index: the difference between consistency values divided by their sum (see Experimental Procedures). For aligned sites (Fig. 3B), the consistency index increased with AGFa microstimulation (median = 0.15, $p < 10^{-4}$, Wilcoxon signed rank test). For nonaligned sites (Fig. 3C), the consistency index decreased with AGFa microstimulation (mean = −0.11, $p < 0.02$, t-test). A similar effect was observed when single trial best ITDs were computed from randomly re-sampled responses to each ITD (see Experimental Procedures). The mean of the consistency index for aligned sites with randomly re-sampled responses to ITD was 0.12 (black arrow in Fig. 3B, $p < 0.0006$, t-test) and for nonaligned sites was −0.13 (black arrow in Fig. 3C, $p< 0.002$). To test whether the changes in tuning consistency can be explained solely by changes in firing rates caused by AGFa microstimulation, we fit the measured mean response rates with a Poisson model. The modeled data exhibited similar changes in the tuning consistency index with AGFa microstimulation (aligned sites: mean change = 0.19, $p = 0.0001$, t-test; nonaligned sites: mean change = −0.14,

$p = 0.0092$). Thus, the changes in tuning consistency caused by AGFa microstimulation can be accounted for by increases and decreases in mean firing rate.

Effect on stimulus discriminability

AGFa microstimulation increased stimulus discriminability at aligned OT sites. Stimulus discriminability is the reliability with which changes in neuronal firing rate indicate changes in stimulus value. We measured stimulus discriminability for unit responses to neighboring values of ITD separated by 10 μs increments (about 4° azimuth). We quantified stimulus discriminability as the change in mean firing rate for the two distributions of responses divided by the joint standard deviation of the two distributions. This metric, called 'standard separation' (Sakitt, 1973), does not saturate, as do other indices of discrimination (such as ROC analysis), and it has been used previously to quantify a relationship between neuronal and behavioral spatial acuity in barn owls (Bala et al., 2003; Bala et al., 2007), allowing us to compare our results with those from earlier studies.

The value for standard separation (D) varied greatly across the receptive field of each OT unit (Fig. 4B). The largest value of D (Dmax) always occurred on the flanks of the tuning curve, (mean difference between Dmax ITD and best ITD = 20 μs ± 15), where changes in mean response rates with changes in ITD were large (Fig 4C–D). For the aligned OT site represented in Fig. 4A, with a best ITD of −38 μs, Dmax was 2.6 for ITDs between −10 and −20 μs (Fig. 4B, black curve). AGFa microstimulation increased Dmax to 4.5 for the same range of ITDs (Fig. 4B, red curve).

We compared Dmax values, measured with and without AGFa microstimulation, across the population of AGFa -OT sites. For most sites, Dmax values resulted from the same ITD interval with and without AGFa stimulation (e.g., Fig. 4B). For some sites (13 out of 57), however, Dmax resulted from different ITD intervals, usually on opposite flanks of the tuning curve. In either case, we used the largest D value from each tuning curve for comparison. For aligned AGFa -OT sites, Dmax increased from an average value of 2 without AGFa microstimulation to a value of 2.25 with AGFa microstimulation ($p < 0.02$, t-test; Fig. 4E). For nonaligned AGFa -OT sites, Dmax values were surprisingly not affected by AGFa microstimulation (Fig. 4F; Dmax without and with AGF microstimulation = 1.7; the lower Dmax values without microstimulation for nonaligned versus aligned sites may reflect the more peripheral locations of nonaligned receptive fields where tuning is less sharp). A Poisson model of mean spike rates for aligned sites without and with AGFa microstimulation yielded similar increases in Dmax ($p = 0.002$, t-test), indicating that the experimentally observed increases in Dmax can be accounted for by the increases in mean response rates caused by AGFa microstimulation.

Discussion

This study demonstrates that electrical microstimulation of the forebrain gaze area in the owl engages two distinct top-down mechanisms: One operates focally to regulate neuronal responsiveness, tuning consistency and spatial resolution specifically at the location represented by the forebrain stimulation site, and another operates globally to regulate response gain to stimuli at other locations. The existence of two different mechanisms has important implications for studies of cellular mechanisms of top-down control, as well as for interpreting and modeling the effects of top-down control on behavioral and neuronal sensitivity in owls and other species. In the discussion that follows, we review the effects that each mechanism exerts on the representation of sensory information in the OT, and we discuss properties of underlying neural mechanisms that could account for these effects. Then, we compare the effects of AGFa microstimulation with similar effects that result from microstimulating the FEF in monkeys. Finally, we consider the implications of these distinct mechanisms for behavioral correlates of spatial attention.

Distinct effects of top-down regulation

Microstimulation of the AGFa enhances the representation of auditory information in the OT in at least four ways. First, it increases the sensitivity of OT neurons with aligned receptive fields to low-level sounds. This effect is functionally equivalent to turning up the level of the sound. Second, AGFa microstimulation increases the consistency with which OT neurons represent the location of a stimulus (Fig. 3). Third, AGFa microstimulation increases the ability of OT neurons to signal a change in the location (ITD) of a stimulus with a change in firing rate (Fig. 4). The increased resolution occurs only for ITDs that are on the flanks of the tuning curves (Fig. 4C). However, AGFa stimulation increases the responsiveness of OT neurons with receptive fields misaligned by as much as ± 9° (± 22 μs ITD) relative to the location represented at the AGFa stimulation site (Winkowski and Knudsen, 2007). Hence, neurons at the edge of this population of OT neurons, with best ITDs that are 20–25 μs away from the best ITD of the AGFa stimulation site, provide increased resolution for ITDs near the best ITD of the AGFa site. Fourth, AGFa microstimulation sharpens auditory receptive fields (width at half-max) at aligned OT sites, thereby increasing their capacity to resolve multiple sound stimuli (Winkowski and Knudsen, 2007).

At the same time that AGFa microstimulation enhances sensitivity and spatial resolution at aligned OT sites, it decreases neuronal responsiveness at nonaligned OT sites. This effect involves a decrease both in the slopes of level-response functions and in the maximum response rates of nonaligned OT neurons, indicating a decrease in response gain. Along with the decrease in gain, there is a decrease in the consistency of spatial tuning (Fig. 3). These suppressive effects extend widely across the OT space map, to neurons tuned at least as far as 30° away from the location represented at the AGFa stimulation site (Winkowski and Knudsen, 2007).

Previous research demonstrates that AGFa microstimulation has similar effects on auditory and visual responsiveness in the OT (Winkowski and Knudsen, 2007). Based on these observations, although neuronal responsiveness in this study was assayed using auditory stimuli, we expect that the effects of AGFa microstimulation on neuronal responsiveness will apply to both sensory modalities.

Mechanisms of top-down regulation

The simultaneous, opposing effects of top-down signals in different regions of the OT space map require the engagement of at least two different mechanisms for controlling neuronal responsiveness, one that operates at aligned sites and another that operates at nonaligned sites.

The mechanisms that are activated at aligned sites in the OT enhance neural sensitivity in ways that are similar to the enhancement of neural sensitivity in the visual cortex of monkeys when they attend voluntarily to stimuli located within the receptive field of a neuron (Reynolds et al., 1999; Womelsdorf et. al., 2006). Converging evidence from various species suggests that the neuromodulator acetylcholine (ACh) may play an important role in the top-down focal enhancement of neuronal sensitivity at aligned sites. First, the OT is intimately interconnected with cholinergic nuclei in the midbrain isthmic complex (analogous to the mammalian parabigeminal nucleus). This connection is reciprocal, topographic and spatially precise (Hunt et al., 1977; Maczko et al., 2006; Wang et al., 2006;). The precision of this cholinergic projection to the OT is consistent with the hypothesis that this pathway provides focal regulation of neuronal responsiveness in the OT. Second, acetylcholine receptors, both nicotinic (nAChRs) and muscarinic, have recently been shown to regulate the responsiveness of visual neurons in the primary visual cortex of monkeys (Disney et al., 2007; Herrero et. al., 2008). The regulation of nAChRs both increases neuronal sensitivity and decreases response thresholds to visual stimuli, in a manner that is similar to the effects of AGFa microstimulation on auditory responses at aligned OT sites reported here. Third, in the primate visual cortex, the

presynaptic localization of nAChRs on thalamic terminals onto glutamatergic cells in layer 4c suggests that activation of nAChRs regulates the effectiveness of sensory input to the cortical circuitry (Disney et al., 2007). As in the visual cortex, nAChRs are dense in the input layers of the OT (Prusky and Cynader, 1988; Sargent et al., 1989;), and pharmacological experiments indicate that the nAChRs act predominantly on presynaptic sensory terminals in the OT (Edwards and Cline, 1999). Moreover, blocking nAChRs in the OT decreases the effectiveness of visual stimulation (Edwards and Cline, 1999). Fourth, in the barn owl OT, the top-down mechanism that enhances neuronal sensitivity also sharpens auditory spatial tuning (Winkowski and Knudsen, 2007). The sharpening of spatial tuning suggests the activation of inhibitory as well as excitatory circuitry, and ACh has been shown to activate both inhibitory and excitatory circuitry in the OT (Endo et al., 2005; Yu and Debski, 2003). Finally, the AGFa sends fibers directly to the cholinergic component of the isthmic complex (Knudsen et al., 1995).

Despite the allure of the cholinergic hypothesis, however, ACh may not act alone in regulating neuronal sensitivity. In the mammalian cerebral cortex, cholinergic fibers from the basal forebrain area do not appear to have the spatial precision required to mediate topographically restricted increases in neuronal sensitivity (Sarter and Bruno, 1997; Sarter et al., 2005). It is possible that top-down glutamatergic projections may interact with cholinergic inputs to provide the requisite spatial precision in the cerebral cortex (Parikh et al, 2008; Disney et al., 2007). In the barn owl midbrain, although the AGFa sends input directly to the cholinergic nuclei in the isthmic complex, the AGFa also sends input directly to the OT (Knudsen et al., 1995; Zeier and Karten, 1971), and this long-distance projection is likely to be glutamatergic. Hence, it is possible that top-down control of focal increases in neuronal sensitivity is mediated by the interaction of cholinergic and glutamatergic inputs in the OT and cortex. This hypothesis remains to be tested.

At the same time that the top-down signal from the AGF activates mechanisms for focal enhancement, it also activates a mechanism that decreases response gain across the rest of the OT. Decreases in response gain have been reported in the monkey visual cortex when monkeys attend to another stimulus (Motter, 1993). A model by Reynolds and Chelazzi (2004) proposes that decreases in response gain to the non-attended stimulus result from increased lateral inhibition caused by the enhanced neural responses to the attended stimulus. This mechanism provides a compelling explanation for the selective suppression of responses to non-attended stimuli when there are two stimuli within a neuron's receptive field, one attended and the other non-attended (Maunsell and Treue, 2006). This mechanism cannot account, however, for the decrease in response gain revealed by our experiments, because we observed a decrease in response gain when gain was tested with a single stimulus. In our experimental paradigm, the "attend-away" condition corresponds to the effect of AGF stimulation on OT responses at nonaligned sites (Fig. 2). Only one stimulus was presented and there was no increase in activity at the site in the OT that corresponds to the location encoded by the AGF stimulation site since AGF stimulation alone did not increase OT activity (see effects of AGFa stimulation on responses to stimuli below threshold in Figs. 1 and 2; Winkowski and Knudsen, 2006; Winkowski and Knudsen, 2007).). Hence, the decrease in response gain, shown in Fig. 2, does not involve responses to a second stimulus. These results indicate instead that top-down signals activate, in addition to the local mechanism proposed by Reynolds and Chelazzi, an additional, global gain-control circuit that does not depend on response enhancement to an attended stimulus.

A circuit in the midbrain that exhibits the requisite properties to mediate gain control globally in the OT is the magnocellular portion of the isthmic complex (Imc). The Imc consists exclusively of GABAergic neurons, suggesting that they inhibit their target neurons (Wang et al., 2004). In addition, Imc neurons receive topographic inputs from the OT and project back

broadly to the OT as well as to the cholinergic portion of the isthmic complex (Wang et al., 2004). As such, they should regulate neuronal excitability across the entire OT and across the entire isthmic complex. Recent experiments involving pharmacological inactivation of the Imc implicate the Imc in competitive interactions in the isthmic complex (Marin et al., 2007). If the Imc does, indeed, mediate gain control in the OT, Imc neurons should be activated by the top-down signal alone and they should exert a divisive effect on the responses of the neurons to which the project. These predictions remain to be tested. Models of attention predict analogous, broadly projecting inhibitory circuits to mediate the effects of spatial attention in the mammalian cortex (Ardid et al., 2007; Itti and Koch, 2001; McDonald and Burkhalter, 1993).

Behavioral correlates of sensitivity and gain control

Measured behaviorally, spatial attention results in increased stimulus detection and discrimination at attended locations and decreased stimulus detection and discrimination at non-attended locations (Lee et al., 1997; Posner, 1980, Yeshurun and Carrasco, 1998, 1999). The two major effects of top-down stimulation on neuronal responsiveness that are characterized in this study correlate with these two kinds of behavioral effects of spatial attention: The focal increase in neuronal sensitivity and spatial resolution at aligned OT sites correlates with improvements in behavioral performance at attended locations (Spitzer et al., 1988; Yeshurun and Carrasco, 1998, 1999), and the global suppression of neuronal responses at nonaligned OT sites correlates with the perceptual suppression of stimuli at non-attended locations (Pestilli and Carrasco, 2005).

The mechanisms for top-down sensitivity and gain control in the OT exert their maximum effects under different stimulus conditions. The focal enhancement of neuronal sensitivity exerts its greatest effects when the signal-to-noise of the stimulus is low and the neurons are operating near threshold. Under these conditions, the top-down signal causes neurons at aligned OT sites to increase their response rates, consistency of tuning, spatial resolution, and 2-point discrimination. These effects are reminiscent of the differential improvement in the detection and discrimination of attended, low-contrast visual stimuli, measured in spatial attention tasks (Martinez-Trujillo and Treue, 2002). On the other hand, the global decrease in response gain for OT neurons representing stimuli at nonaligned locations exerts its greatest effects when nonaligned stimuli are strong. This effect is reminiscent of the increasing benefit that spatial attention affords as the strength of distracting stimuli increases. Thus, as with the benefits of spatial attention, the full benefits of the combined actions of these two mechanisms are realized under conditions of low signal-to-noise target stimuli in the presence of strong, distracting stimuli.

Experiments in barn owls have demonstrated a relationship between auditory spatial acuity, measured behaviorally, and maximum stimulus discriminability (D), measured neurophysiologically in the midbrain (Bala et al., 2003; Bala et al., 2007). Our finding that maximum stimulus discriminability in the OT increases with AGFa microstimulation suggests that top-down stimulation may also increase auditory spatial acuity in behaving owls. In addition, the sharpening of auditory receptive fields that results from AGFa microstimulation, an effect reminiscent of the sharpening of V4 visual receptive fields observed when monkeys attend voluntarily to stimuli in a neuron's receptive field (Spitzer et al, 1988), suggests an increased behavioral capacity to resolve multiple sound sources that is under top-down control.

Gain versus sensitivity

Research in the visual cortex of behaving monkeys engaged in spatial attention tasks has documented changes in neuronal response gain in some studies and changes in neuronal sensitivity in others (Martinez-Trujillo and Treue, 2002; Reynolds et al., 2000; Williford and

Maunsell, 2006). There is debate about which of these effects best characterizes the effects of attention on neuronal responsiveness. The results presented here demonstrate that both of these effects occur in the OT and that they operate simultaneously, in a coordinated push-pull fashion, on complementary portions of the OT space map. As a result, this top-down signal alters *both* the sensitivity and the gain of neuronal responsiveness as the location encoded by the top-down signal shifts to or away from the location encoded by the sensory neurons (Fig. 5).

We hypothesize that equivalent top-down mechanisms operate in the cerebral cortex as well, and that previous neurophysiological experiments on behaving monkeys did not recognized these different mechanisms, because the effects of attention were assessed as the difference in neuronal responses between the attend-toward and attend-away conditions, which necessarily combined their effects. If this hypothesis is true, then in the quest for understanding top-down regulation of sensory responses, at least two, functionally complementary mechanisms for controlling neuronal responsiveness must be sought and modeled: one mechanism that operates focally to regulate neuronal sensitivity and another that operates globally to regulate neuronal gain.

Experimental Procedures

Animals and surgical preparation

A total of 18 barn owls were used in this study. Surgical and experimental procedures were approved by the Stanford University Institutional Animal Care and Use Committee and were in accordance with the National Institutes of Health and Society for Neuroscience guidelines.

Owls were prepared for multiple electrophysiological experiments as described previously (Winkowski and Knudsen, 2007). On the day of an experiment, the owl was anesthetized with halothane (1.5%) and a mixture of nitrous oxide and oxygen (45:55) and was placed in a restraining tube in a prone position within a sound-attenuating booth. The head was secured to a stereotaxic device, and the visual axes were aligned relative to a calibrated tangent screen (the eyes of the owl are nearly stationary in the head). Owls were maintained throughout the experiment in a passive, sedated state with a mixture of nitrous oxide and oxygen.

Auditory stimulation

Auditory stimuli were generated using customized MATLAB (Mathworks) software (courtesy of J. Bergan) interfaced with Tucker Davis Technologies hardware (RP2). Auditory stimuli were delivered through matched earphones (Knowles Electronics, ED-1914) coupled to damping assemblies (BF-1743) inserted into the ear canals ~5 mm from the eardrum. The amplitude and phase spectra of the two earphones were equalized to within ±2 dB and ±2 μs, respectively. Auditory tuning was measured by presenting dichotic noise bursts (100 or 250 ms duration, 2–10 kHz, 0 ms rise/fall times, 10–20 dB above unit threshold; interstimulus interval = 1.2 sec). Tuning to interaural timing differences (ITDs) and interaural level differences (ILDs) was assessed by presenting 10–20 series of noise bursts with ITD (or ILD) varied in a random, interleaved fashion while ILD (or ITD) was held constant at the best value for the site.

Neurophysiology

Epoxy-coated tungsten microelectrodes (0.5 – 2 MΩ at 1-kHz) were used to record extracellularly from single and multiple units (sites) in the AGF and OT and to deliver electrical microstimulation to the AGF. We studied the effects of AGF microstimulation on the responses of single or multiple units in the deep layers (layers 11–13) of the OT. In most experiments, we studied the effect of a single AGF site on responses at more than one OT recording site by advancing the recording electrode to new position in the OT. Spike times were saved on a

computer using TDT hardware (RA-16) controlled by customized MATLAB (Mathworks) software.

AGF microstimulation

The AGF was identified based on stereotaxic coordinates and functional properties. Electrical stimulation was delivered to the AGF site through a tungsten microelectrode (0.5 – 1.0 MΩ at 1-kHz). Stimulation waveforms were generated with a Grass stimulator (S88) and two Grass stimulus isolation units (PSIU-6). The waveforms consisted of 25 ms trains of biphasic current pulses, 200-Hz, and 200 μs phase duration. The electrical stimulation trains were timed so that they just preceded unit discharges elicited by sensory stimulation.

For each AGF stimulation site, the current threshold to evoke an eye saccade was determined by incrementally increasing the stimulation current until a small amplitude saccadic eye movement (a deflection in the position of a retinal landmark, the pecten oculus, viewed ophthalmoscopically) was observed. Once the threshold for eliciting an eye saccade from an AGF site was determined, the amplitude of the current pulses was set to a low level (usually 5 μA) and incrementally increased until either an effect on OT auditory responses was observed or the current amplitude reached 40 μA; the lowest current level that evoked an eye saccade was 55 μA.

Data analysis

Net responses at each OT site were quantified by subtracting the average firing rate that occurred during the 100 ms interval prior to the onset of electrical microstimulation across all trials (baseline activity) from the average firing rate occurring during a 100 ms window beginning 5 ms following the offset of the electrical stimulus. This window was chosen to avoid contamination of the data by the stimulation artifact. Identical post-stimulus periods were sampled for trials during which electrical microstimulation was and was not applied to the AGF site. Trials in which the AGFa was microstimulated alone were interleaved with these trials. Net firing rate across all trials for a single condition was averaged. Paired t-tests were used to compare the firing rates for trials with and without microstimulation. Auditory best ITD and best ILD were quantified as the weighted average of responses that were greater than half of the maximum response (half-max). Tuning widths were defined as the continuous range of ITDs or ILDs that elicited responses greater than half-max. Response thresholds were quantified as the minimum sound level, at best ITD and best ILD, required to elicit a response greater than twice the standard deviation of baseline activity.

ABL curves—To determine the effect of AGF microstimulation on sound level-response functions in the OT, we measured OT responses to sounds presented at the best ITD and best ILD for each site, across a wide range of average binaural levels (ABL), with and without AGF microstimulation. The ABL of each stimulus was selected at random from a set of at least 7 sound levels. To characterize the sound level-response functions, we used a least squares fit of a hyperbolic ratio function to the mean responses:

$$r = r_{\max} \bullet \left(\frac{c^n}{c^n + c_{50}^n}\right) + m$$

where r is the neuronal response, c is the sound level, r_{max} is the maximum response, m is the spontaneous discharge rate, c_{50} is the sound level at which the response reached half-max, and n is an exponent that determines the steepness of the response function. This function has been shown to provide a good fit to contrast-response functions measured in the visual cortex of cats and monkeys (Martinez-Trujillo and Treue, 2002; Williford and Maunsell, 2006). To

assess the effect of AGF microstimulation on each parameter of the sound level-response function, we

$$M.I.=\frac{(P_{stim}-P_{nostim})}{(P_{stim}+P_{nostim})}$$

computed a modulation index:

where P_{stim} is the value of the parameter when the AGF was stimulated and P_{nostim} is the value of the parameter when the AGF was not stimulated.

Data from all sites were included for the population analyses. Population level response functions were constructed for each test by normalizing the mean firing rate for each OT site to the maximum mean firing rate for that site measured without AGF stimulation. All sound level response functions were aligned according to the threshold value (plotted as ABL = 0 dB) and averaged.

Response consistency was determined by computing the Fano factor (variance of spike count/mean spike count) of responses to the best ITD, with and without AGFa microstimulation. We compared the distributions of Fano factor using a modulation index (see above) and determined whether the distribution of Fano factor index values was different from zero.

Tuning consistency was determined by computing the reciprocal of the variance of the best ITDs across a set of trials (> 15 repetitions of each stimulus set) with and without AGFa microstimulation. At individual sites, the variances of the distributions of the best ITDs with and without AGFa microstimulation were compared using a two-sample F-test for equal variance. Across the population, the change in consistency was determined by constructing a consistency index where the difference between the consistency values was divided by their sum. In addition, we randomly sampled the response data generated for each ITD value across all repetitions and calculated the best ITD from each randomly generated sample with and without AGFa microstimulation. We repeated this 100 times, yielding 100 values of best ITD with and without AGFa microstimulation. Consistency values (reciprocal of the variance of best ITDs) were determined for the re-sampled best ITDs and a consistency index was constructed.

Stimulus discrimination was computed by assessing the change in ring rates evoked by neighboring values of ITD differing by 10 μs (about 4° azimuth) using a metric referred to as standard separation (Sakitt, 1973). This metric is quantified as the difference in the means divided by the joint standard deviations:

$$D=\frac{\mu_1-\mu_2}{\sqrt{\delta_1\delta_2}}$$

where μ_1 is the mean firing rate at ITD_1 and μ_2 is the mean firing rate at ITD_2 ($\Delta ITD = 10$ μs) and δ_1 and δ_2 are the standard deviations of the firing rates at ITD_1 and ITD_2, respectively. ITD tuning was measured at either 10 or 20 μs intervals. We used the spline function to generate interpolated neural response values. We then computed the values of the standard separation (D) with and without AGFa microstimulation for the entire tuning curve using the interpolated response values from the spline fits. The maximum value of D (Dmax) was found for the discrimination curve with and without AGFa microstimulation ($Dmax_{stim}$ and $Dmax_{nostim}$, respectively).

Acknowledgements

We thank members of the Knudsen lab for critical discussion throughout all phases of the research, and P. Knudsen for expert technical assistance. This research was supported by NIH grants F32DC006569 (D.W.) and R01DC000155 (E.K.).

References

Albrecht DG, Hamilton DB. Striate cortex of monkey and cat: contrast response function. J Neurophysiol 1982;48:217–237. [PubMed: 7119846]

Ardid S, Wang XJ, Compte A. An integrated microcircuit model of attentional processing in the neocortex. J Neurosci 2007;27:8486–8495. [PubMed: 17687026]

Armstrong KM, Fitzgerald JK, Moore T. Changes in visual receptive fields with microstimulation of frontal cortex. Neuron 2006;50:791–798. [PubMed: 16731516]

Armstrong KM, Moore T. Rapid enhancement of visual cortical response discriminability by microstimulation of the frontal eye field. Proc Natl Acad Sci U S A 2007;104:9499–9504. [PubMed: 17517599]

Bala AD, Spitzer MW, Takahashi TT. Prediction of auditory spatial acuity from neural images on the owl's auditory space map. Nature 2003;424:771–774. [PubMed: 12917684]

Bala AD, Spitzer MW, Takahashi TT. Auditory spatial acuity approximates the resolving power of space-specific neurons. PLoS ONE 2007;2:e675. [PubMed: 17668055]

Bauer M, Oostenveld R, Peeters M, Fries P. Tactile spatial attention enhances gamma-band activity in somatosensory cortex and reduces low-frequency activity in parieto-occipital areas. J Neurosci 2006;26:490–501. [PubMed: 16407546]

Cohen YE, Knudsen EI. Binaural tuning of auditory units in the forebrain archistriatal gaze fields of the barn owl: local organization but no space map. J Neurosci 1995;15:5152–5168. [PubMed: 7623142]

Desimone R, Duncan J. Neural mechanisms of selective visual attention. Annu Rev Neurosci 1995;18:193–222. [PubMed: 7605061]

Dias EC, Segraves MA. Muscimol-induced inactivation of monkey frontal eye field: effects on visually and memory-guided saccades. J Neurophysiol 1999;81:2191–2214. [PubMed: 10322059]

Disney AA, Aoki C, Hawken MJ. Gain modulation by nicotine in macaque v1. Neuron 2007;56:701–713. [PubMed: 18031686]

Edwards JA, Cline HT. Light-induced calcium influx into retinal axons is regulated by presynaptic nicotinic acetylcholine receptor activity in vivo. J Neurophysiol 1999;81:895–907. [PubMed: 10036287]

Endo T, Yanagawa Y, Obata K, Isa T. Nicotinic acetylcholine receptor subtypes involved in facilitation of GABAergic inhibition in mouse superficial superior colliculus. J Neurophysiol 2005;94:3893–3902. [PubMed: 16107532]

Fritz JB, Elhilali M, David SV, Shamma SA. Auditory attention--focusing the searchlight on sound. Curr Opin Neurobiol 2007;17:437–455. [PubMed: 17714933]

Herrero JL, Roberts MJ, Delicato LS, Gieselmann MA, Dayan P, Thiele A. Acetylcholine contributes through muscarinic receptors to attentional modulation in V1. Nature. 2008

Hoffman JE, Subramaniam B. The role of visual attention in saccadic eye movements. Percept Psychophys 1995;57:787–795. [PubMed: 7651803]

Hunt SP, Streit P, Kunzle H, Cuenod M. Characterization of the pigeon isthmo-tectal pathway by selective uptake and retrograde movement of radioactive compounds and by Golgi-like horseradish peroxidase labeling. Brain Res 1977;129:197–212. [PubMed: 69469]

Itti L, Koch C. Computational modelling of visual attention. Nature Rev Neurosci 2001;2:194–203. [PubMed: 11256080]

Kauramäki J, Jääskeläinen IP, Sams M. Selective attention increases both gain and feature selectivity of the human auditory cortex. PLoS ONE 2007;2:e909. [PubMed: 17878944]

Knudsen EI, Knudsen PF. Disruption of auditory spatial working memory by inactivation of the forebrain archistriatum in barn owls. Nature 1996;383:428–431. [PubMed: 8837773]

Knudsen EI, Cohen YE, Masino T. Characterization of a forebrain gaze field in the archistriatum of the barn owl: microstimulation and anatomical connections. J Neurosci 1995;15:5139–5151. [PubMed: 7623141]

Knudsen EI. Fundamental components of attention. Annu Rev Neurosci 2007;30:57–78. [PubMed: 17417935]

Lee DK, Koch C, Braun J. Spatial vision thresholds in the near absence of attention. Vision Res 1997;37:2409–2418. [PubMed: 9381676]

Maczko KA, Knudsen PF, Knudsen EI. Auditory and visual space maps in the cholinergic nucleus isthmi pars parvocellularis of the barn owl. J Neurosci 2006;26:12799–12806. [PubMed: 17151283]

Marin G, Salas C, Sentis E, Rojas X, Letelier JC, Mpodozis J. A cholinergic gating mechanism controlled by competitive interactions in the optic tectum of the pigeon. J Neurosci 2007;27:8112–8121. [PubMed: 17652602]

Martinez-Trujillo J, Treue S. Attentional modulation strength in cortical area MT depends on stimulus contrast. Neuron 2002;35:365–370. [PubMed: 12160753]

Maunsell JH, Cook EP. The role of attention in visual processing. Philos Trans R Soc Lond B Biol Sci 2002;357:1063–1072. [PubMed: 12217174]

Maunsell JH, Treue S. Feature-based attention in visual cortex. Trends Neurosci 2006;29:317–322. [PubMed: 16697058]

McDonald CT, Burkhalter A. Organization of long-range inhibitory connections with in rat visual cortex. J Neurosci 1993;13:768–781. [PubMed: 7678860]

McPeek RM, Keller EL. Deficits in saccade target selection after inactivation of superior colliculus. Nat Neurosci 2004;7:757–763. [PubMed: 15195099]

Medina L, Reiner A. Distribution of choline acetyltransferase immunoreactivity in the pigeon brain. J Comp Neurol 1994;342:497–537. [PubMed: 8040363]

Moore T, Armstrong KM. Selective gating of visual signals by microstimulation of frontal cortex. Nature 2003;421:370–373. [PubMed: 12540901]

Moore T, Armstrong KM, Fallah M. Visuomotor origins of covert spatial attention. Neuron 2003;40:671–683. [PubMed: 14622573]

Moore T, Fallah M. Control of eye movements and spatial attention. Proc Natl Acad Sci U S A 2001;98:1273–1276. [PubMed: 11158629]

Moore T, Fallah M. Microstimulation of the frontal eye field and its effects on covert spatial attention. J Neurophysiol 2004;91:152–162. [PubMed: 13679398]

Moran J, Desimone R. Selective attention gates visual processing in the extrastriate cortex. Science 1985;229:782–784. [PubMed: 4023713]

Motter BC. Focal attention produces spatially selective processing in visual cortical areas V1, V2, and V4 in the presence of competing stimuli. J Neurophysiol 1993;70:909–919. [PubMed: 8229178]

Muller JR, Philiastides MG, Newsome WT. Microstimulation of the superior colliculus focuses attention without moving the eyes. Proc Natl Acad Sci U S A 2005;102:524–529. [PubMed: 15601760]

Olsen JF, Knudsen EI, Esterly SD. Neural maps of interaural time and intensity differences in the optic tectum of the barn owl. J Neurosci 1989;9:2591–2605. [PubMed: 2746340]

Parikh V, Man K, Decker MW, Sarter M. CGlutamatergic contributions to nicotinic acetylcholine receptor agonist-evoked cholinergic transients in the prefrontal cortex. J Neurosci 2008;28:3769–3780. [PubMed: 18385335]

Pestilli F, Carrasco M. Attention enhances contrast sensitivity at cued and impairs it at uncued locations. Vision Res 2005;45:1867–1875. [PubMed: 15797776]

Posner MI. Orienting of attention. Q J Exp Psychol 1980;32:3–25. [PubMed: 7367577]

Prusky GT, Cynader MS. [3H]nicotine binding sites are associated with mammalian optic nerve terminals. Vis Neurosci 1988;1:245–248. [PubMed: 3154797]

Reynolds JH, Chelazzi L, Desimone R. Competitive mechanisms subserve attention in macaque areas V2 and V4. J Neurosci 1999;19:1736–1753. [PubMed: 10024360]

Reynolds JH, Chelazzi L. Attentional modulation of visual processing. Annu Rev Neurosci 2004;27:611–647. [PubMed: 15217345]

Reynolds JH, Pasternak T, Desimone R. Attention increases sensitivity of V4 neurons. Neuron 2000;26:703–714. [PubMed: 10896165]

Sakitt B. Indices of discriminability. Nature 1973;241:133–134. [PubMed: 4695543]

Sargent PB, Pike SH, Nadel DB, Lindstrom JM. Nicotinic acetylcholine receptor-like molecules in the retina, retinotectal pathway, and optic tectum of the frog. J Neurosci 1989;9:565–573. [PubMed: 2645388]

Sarter M, Bruno JP. Cognitive functions of cortical acetylcholine: toward a unifying hypothesis. Brain Res Brain Res Rev 1997;23:28–46. [PubMed: 9063585]

Sarter M, Hasselmo ME, Bruno JP, Givens B. Unraveling the attentional functions of cortical cholinergic inputs: interactions between signal-driven and cognitive modulation of signal detection. Brain Res Brain Res Rev 2005;48:98–111. [PubMed: 15708630]

Shepherd M, Findlay JM, Hockey RJ. The relationship between eye movements and spatial attention. Q J Exp Psychol A 1986;38:475–491. [PubMed: 3763952]

Spitzer H, Desimone R, Moran J. Increased attention enhances both behavioral and neuronal performance. Science 1988;240:338–340. [PubMed: 3353728]

Steinmetz PN, Roy A, Fitzgerald PJ, Hsiao SS, Johnson KO, Niebur E. Attention modulates synchronized neuronal firing in primate somatosensory cortex. Nature 2000;404:187–190. [PubMed: 10724171]

Swanson LW, Simmons DM, Whiting PJ, Lindstrom J. Immunohistochemical localization of neuronal nicotinic receptors in the rodent central nervous system. J Neurosci 1987;7:3334–3342. [PubMed: 2822866]

Wang Y, Luksch H, Brecha NC, Karten HJ. Columnar projections from the cholinergic nucleus isthmi to the optic tectum in chicks (Gallus gallus): a possible substrate for synchronizing tectal channels. J Comp Neurol 2006;494:7–35. [PubMed: 16304683]

Wang Y, Major DE, Karten HJ. Morphology and connections of nucleus isthmi pars magnocellularis in chicks (Gallus gallus). J Comp Neurol 2004;469:275–297. [PubMed: 14694539]

Williford T, Maunsell JH. Effects of spatial attention on contrast response functions in macaque area V4. J Neurophysiol 2006;96:40–54. [PubMed: 16772516]

Winkowski DE, Knudsen EI. Top-down gain control of the auditory space map by gaze control circuitry in the barn owl. Nature 2006;439:336–339. [PubMed: 16421572]

Winkowski DE, Knudsen EI. Top-down control of multimodal sensitivity in the barn owl optic tectum. J Neurosci 2007;27:13279–13291. [PubMed: 18045922]

Womelsdorf T, Anton-Erxleben K, Pieper F, Treue S. Dynamic shifts of visual receptive fields in cortical area MT by spatial attention. Nat Neurosci 2006;9:1156–1160. [PubMed: 16906153]

Woodson W, Reiner A, Anderson K, Karten HJ. Distribution, laminar location, and morphology of tectal neurons projecting to the isthmo-optic nucleus and the nucleus isthmi, pars parvocellularis in the pigeon (Columba livia) and chick (Gallus domesticus): a retrograde labelling study. J Comp Neurol 1991;305:470–488. [PubMed: 1709956]

Yeshurun Y, Carrasco M. Attention improves or impairs visual performance by enhancing spatial resolution. Nature 1998;396:72–75. [PubMed: 9817201]

Yeshurun Y, Carrasco M. Spatial attention improves performance in spatial resolution tasks. Vision Res 1999;39:293–306. [PubMed: 10326137]

Yu CJ, Debski EA. The effects of nicotinic and muscarinic receptor activation on patch-clamped cells in the optic tectum of rana pipiens. Neuroscience 2003;118:135–144. [PubMed: 12676145]

Zeier H, Karten HJ. The archistriatum of the pigeon: organization of afferent and efferent connections. Brain Res 1971;31:313–326. [PubMed: 5569153]

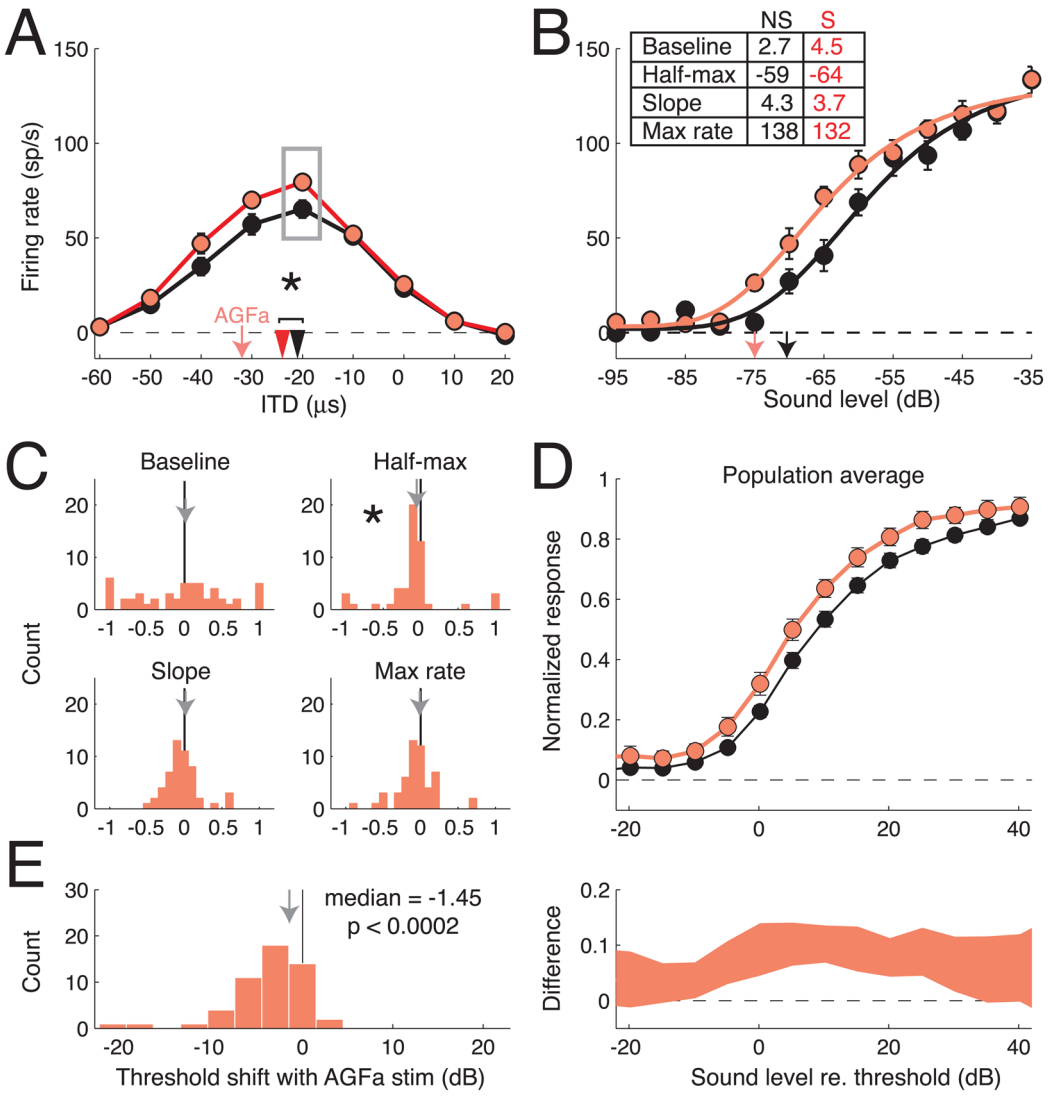

Figure 1.

Effects of AGFa microstimulation on OT auditory responses at aligned AGFa-OT sites. A) Mean firing rate for the OT site plotted as a function of stimulus ITD for trials with (red) and without (black) AGFa microstimulation. Error bars represent s.e.m. Black arrowhead: best $ITD_{no\ stim} = -21$ µs; red arrowhead: best $ITD_{stim} = -23$ µs; red arrow: best ITD of the AGFa stimulation site = −32 µs. B) Mean firing rate and best-fit sound level response functions with (red) and without (black) AGFa microstimulation. Responses are to sounds with best ITD and best ILD values for this site. Error bars represent s.e.m. Parameters of the fitted curves with and without microstimulation (S and NS, respectively) are indicated in the upper left. C) Effects of AGFa microstimulation on the fits of sound level response functions to the response data. For each of the 4 sound level response function parameters (r_{max}, m, c_{50}, and n; see Experimental Procedures), the change between parameters with and without AGFa microstimulation was converted to a modulation index (see Experimental Procedures). Each panel plots the distribution of modulation indices across the population. Arrows mark the mean modulation index. The distribution of indices was significantly different from zero for only c_{50} (asterisk). D) *Top:* Population ABL curves measured with (red circles and line) and without (black circles and line) AGFa microstimulation. Ordinate shows normalized response; abscissa

shows stimulus ABL normalized to the threshold ABL without AGFa stimulation (plotted as ABL = 0 dB). In most cases, error bars are smaller than the symbol. *Bottom:* Difference in the normalized sound level response functions measured with versus without AGFa microstimulation plotted as a function of sound level. Responses to sounds that were 5 dB below threshold to 25 dB above were significantly increased by AGFa microstimulation. E) Distribution of the changes in response threshold with AGFa microstimulation (see Experimental Procedures). Distribution is shifted toward negative values indicating that responses could be driven by lower sound levels with AGFa microstimulation. The median value of the distribution is −1.45 dB.

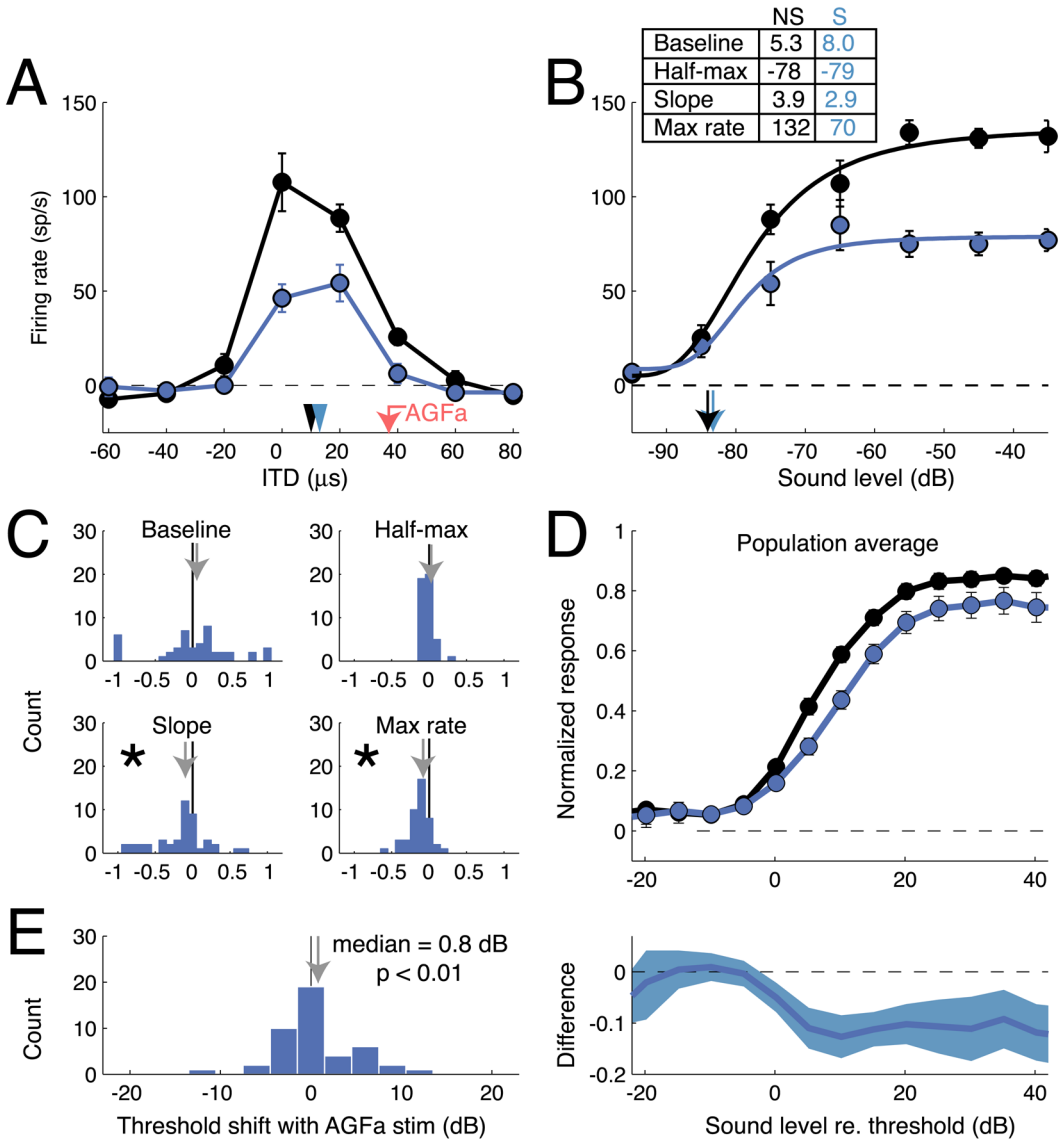

Figure 2.

Effects of AGFa microstimulation at nonaligned AGFa-OT sites. Conventions are the same as in Fig. 1. A) Mean firing rate of the OT site plotted as a function of stimulus ITD for trials with (blue) and without (black) AGFa microstimulation. Error bars represent s.e.m. Black arrowhead: best $ITD_{no\ stim}$ = +10 μs; blue arrowhead: best ITD_{stim} = +13 μs; red arrow: best ITD of the AGFa stimulation site = +38 μs. B) Mean firing rate and best-fit sound level response functions with (blue) and without (black) AGFa microstimulation. Responses are to a sound with the best ITD and best ILD values for this site. Error bars represent ± 1 s.e.m. Parameters of the fitted curves are indicated in the upper left. C) Effects of AGFa microstimulation on sound level response functions fit to the response data at nonaligned sites. Each panel plots the distribution of modulation indices across the population, with arrows marking the mean modulation index. The mean modulation index was significantly different from zero for *n* and r_{max} (asterisks). D) *Top:* Population ABL curves measured with (blue circles and line) and without (black circles and line) AGFa microstimulation. Ordinate shows normalized response; abscissa shows stimulus ABL normalized to the threshold ABL without AGFa stimulation

(plotted as ABL = 0 dB). In most cases, errorbars are smaller than the symbol. *Bottom:* Difference in the normalized sound level response functions measured with versus without AGFa microstimulation. Significant suppression of responses was observed for responses to sound levels at and above threshold. E) Distribution of the changes in response threshold with AGFa microstimulation. Distrbution is shifted toward positive values indicating that higher sound levels were required to drive responses with AGFa microstimulation. The median value of the distribution is +0.8 dB.

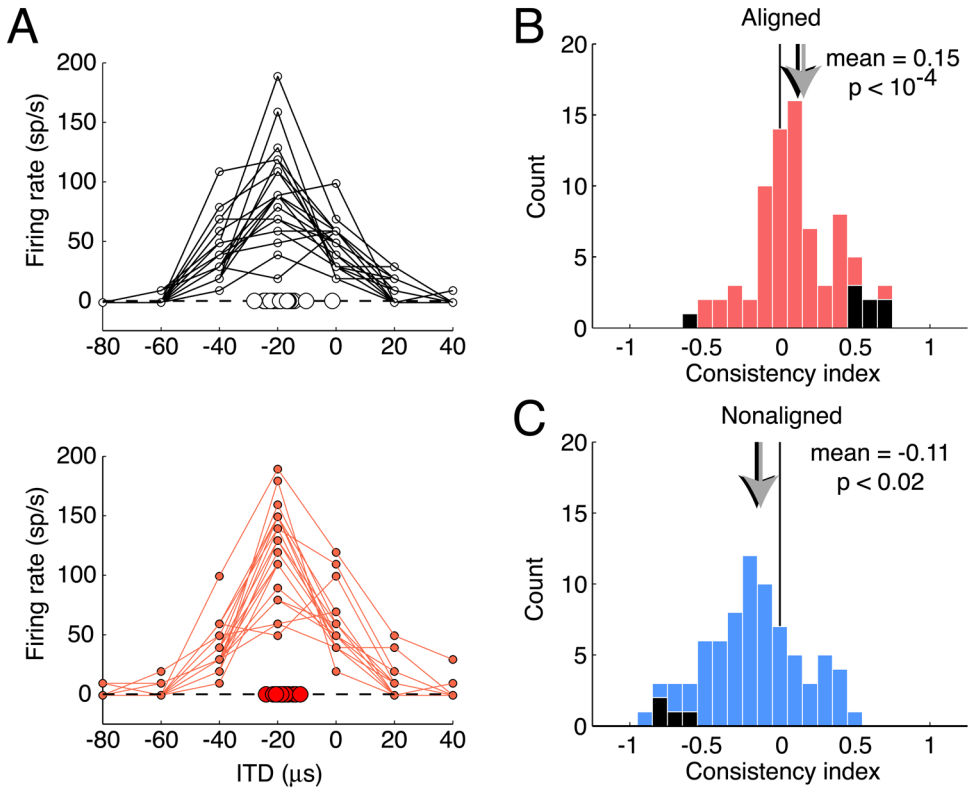

Figure 3.

Effect of AGFa microstimulation on tuning consistency at aligned and nonaligned sites. A) Top: Firing rate as a function of stimulus ITD for trials without AGFa microstimulation. Each line represents the firing rates evoked (ordinate) to a range of stimulus ITDs (abscissa) on a repetition of a complete set of ITD values. Open circles along abscissa represent the best ITDs (see Experimental Procedures) calculated for each repetition. Bottom: Firing rate as a function of stimulus ITD for trials with AGFa microstimulation. Conventions are the same as in Top. B) Distribution of consistency indices for aligned sites (see Experimental Procedures). The distribution is shifted toward positive values indicating that the tuning of OT sites became more consistent with AGFa microstimulation. Black bars indicate individual sites at which a significant difference in tuning variance was observed. C) Distribution of consistency indices for nonaligned sites. The distribution is shifted toward negative values indicating that the tuning of OT sites became less consistent with AGFa microstimulation. Black bars indicate individual sites at which a significant difference in tuning variance was observed.

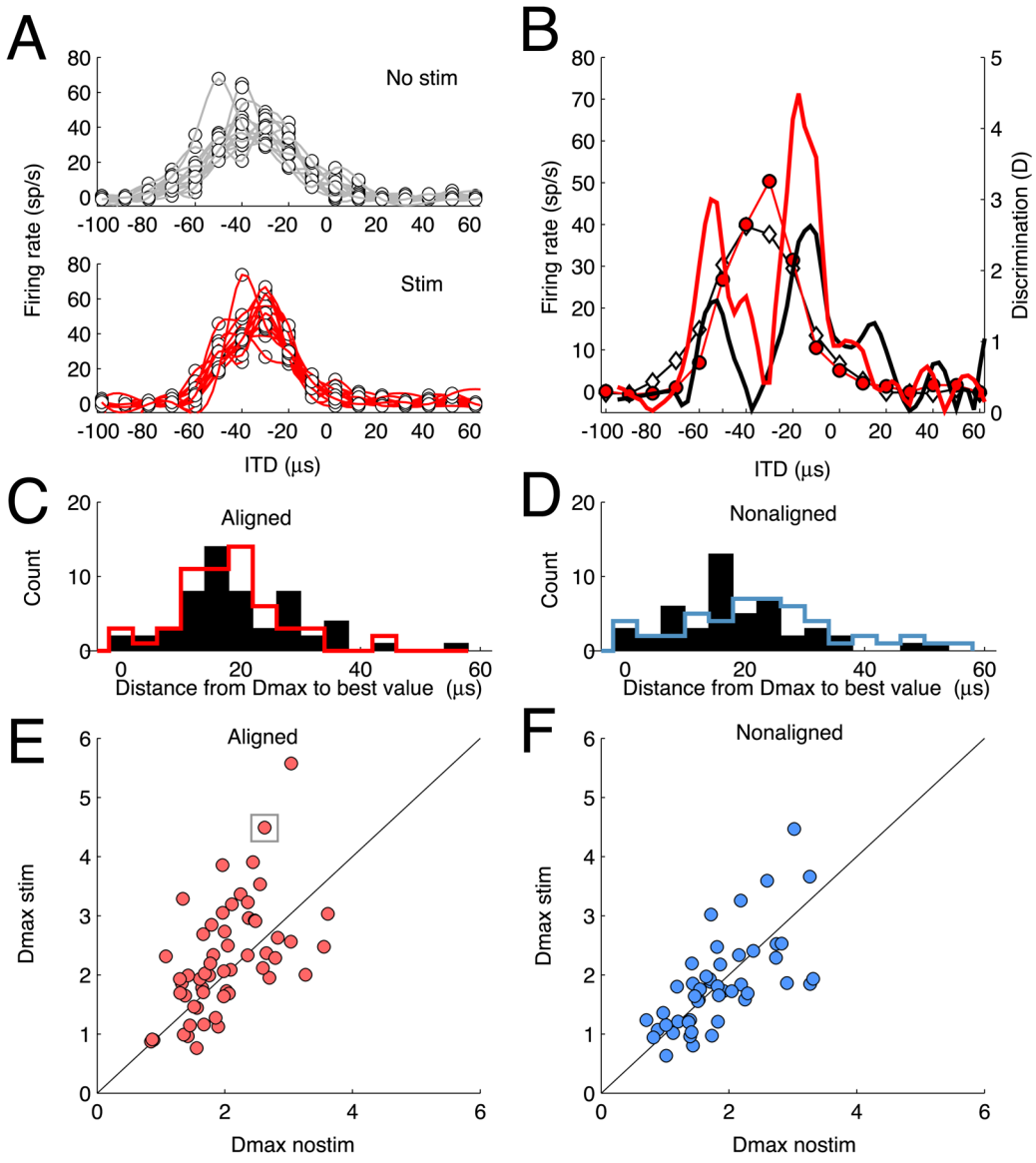

Figure 4.

Effect of AGFa microstimulation on stimulus discrimination at aligned and nonaligned sites. A) Top: Firing rate as a function of stimulus ITD for trials without AGFa microstimulation. Each dot represents the firing rate evoked (ordinate) in response to the corresponding stimulus ITD (abscissa); each thin line represents the spline-fit to the firing rates evoked on a single repetition of a complete set of ITD values. Bottom: Firing rate as a function of stimulus ITD for trials with AGFa microstimulation. Conventions are the same as for Top. B) Comparison of ITD tuning and calculated values of D with (red) and without (black) AGFa microstimulation; the data are from the same site as in A. The average spline-fits to the response data with (red lines and circles) and without (black lines and white diamonds) AGFa microstimulation are plotted in the background ($Dmax_{nostim}$ = 2.6; $Dmax_{stim}$ = 4.5. C). Distribution of absolute differences between best ITD and Dmax ITD for aligned sites. Black bars: histogram of differences from best ITD to Dmax ITD without AGFa microstimulation; Red line: histogram of differences from best ITD to Dmax ITD with AGFa microstimulation. These distributions were not different ($p > 0.5$, t-test). D) Distribution of absolute differences

between best ITD and Dmax ITD for nonaligned sites. Conventions the same as in C. Black bars: histogram of differences from best ITD to Dmax ITD without AGFa microstimulation; Red line represents the histogram of differences from best ITD to Dmax ITD with AGFa microstimulation. These distributions were not different ($p > 0.5$, t-test). E) Scatter plot comparing Dmax values with and without AGFa microstimulation for aligned sites. Ordinate: $Dmax_{stim}$; abscissa: $Dmax_{nostim}$. Each symbol represents one OT site; the boxed symbol indicates data for the site shown in A and B. The diagonal line represents equal values of Dmax with and without AGFa microstimulation. F) Scatter plot comparing Dmax values with and without AGFa microstimulation for nonaligned sites; plotted as described for C.

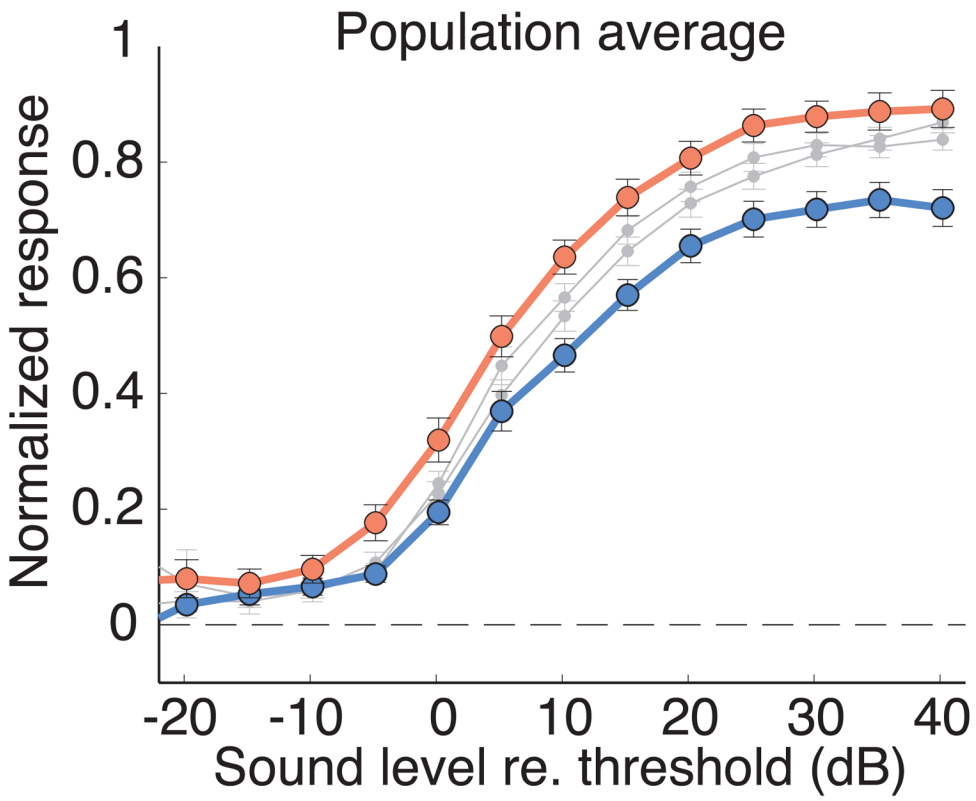

Figure 5.

Overall effect of AGFa microstimulation on neural gain and sensitivity in the OT. The red curve is the population average, level-response function with AGFa stimulation at aligned sites (from Fig. 1D), and the blue curve is the population average, level-response function with AGFa stimulation at nonaligned sites (from Fig. 2D). Gray curves are the average level-response functions without AGFa stimulation. The blue curve is analogous to “attend away”; the red curve is analogous to “attend toward”.